

Supporting Information

Super-hydrophobic Film Retards Frost Formation

Min He^{1,2}, Jingxia Wang¹, Huiling Li¹, Xiaoling Jin¹, Biqian Liu^{1*}, Yanlin Song^{1,3*}

Materials. isotactic polypropylene (i-PP) was purchased from Beijing Yanshan petrochemical Co., Ltd. with a weight-average molecular weight (M_w) of 4.15×10^5 and a polydispersity index $M_w/M_n = 1.41$ (measured using a Waters alliance GPC 2000). P-xylene and methyl ethyl ketone (MEK) were provided by Beijing Beihua Fine Chemical Co., Ltd.

The fabrication of hydrophobic i-PP film. i-PP was placed between two clean glass slides and melted at 200 °C. The melted i-PP was pressed into thin film and then the thin i-PP film was cooled and peered from the glasses.

The fabrication of super-hydrophobic i-PP film. i-PP was dissolved in mixed solvent of p-xylene and MEK (60:40 in volume) at 135 °C to form solution of 30 mg/ml. A few drops of the polymer solution were dropped onto an aluminium foil which has high thermal conductivity, and finally the polymer solution on the aluminium foil was dried under vacuum at room temperature.

In-Situ observations of frost formation on the hydrophobic and super-hydrophobic surface.

The processes of frost formation on the i-PP films were observed using CA System OCA40 (Dataphysics Co., Germany) with a maximum magnification of $\times 2000$ as microscopic image system (Fig. S1). Humidity controller (Beijing YaDu Technical Company for Cleaning Air, Ltd.) is used to control the relative humidity. The surface temperature of the cold plate was tested precisely by 4 T-type thermocouples, recorded by a temperature data acquisition system (Beijing Zhongxin Sci-Tech. Co., Ltd.) and averaged as the surface temperature. The process of frost

formation was recorded by the microscopic image system at a speed of 25 f/s. The hydrophobic and super-hydrophobic films were maintained at $-10\text{ }^{\circ}\text{C}$ and relative humidity (RH) of 50%. The same experiment was examined at other condition (for example, $-14\text{ }^{\circ}\text{C}$ and RH 30%) and showed in Fig. S2, Fig. S3 and Fig. S4.

Characterization. Morphologies of the i-PP films were characterized by Field Emission Scanning Electron Microscopy (FESEM JSM-6700 JEOL Co. Jap). The static water contact angle (CA) and slide water CA were obtained with CA System OCA20 (Dataphysics Co., Germany). The water contact angles (CAs) of the condensed water droplet on the hydrophobic and super-hydrophobic film were obtained with CA System OCA40. In the course of frost formation, the water CAs of the typical condensed water droplets were collected every 1 s until the condensed droplets froze. On the hydrophobic i-PP film the first data was taken from 31 s when the condensed droplet was big enough to be measured. On the super-hydrophobic i-PP film, the first data was taken from 310 s because the condensed droplets merged to form a bigger one.

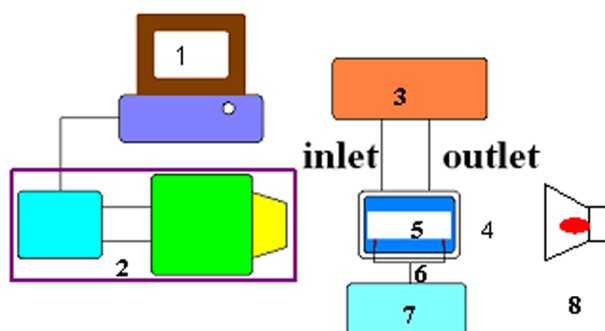


Fig. S1. Experimental apparatus and system: (1) computer; (2) OCA40; (3) antifreeze source; (4) cold plate; (5) sample; (6) T type thermocouples; (7) temperature acquisition system; (8) light source.

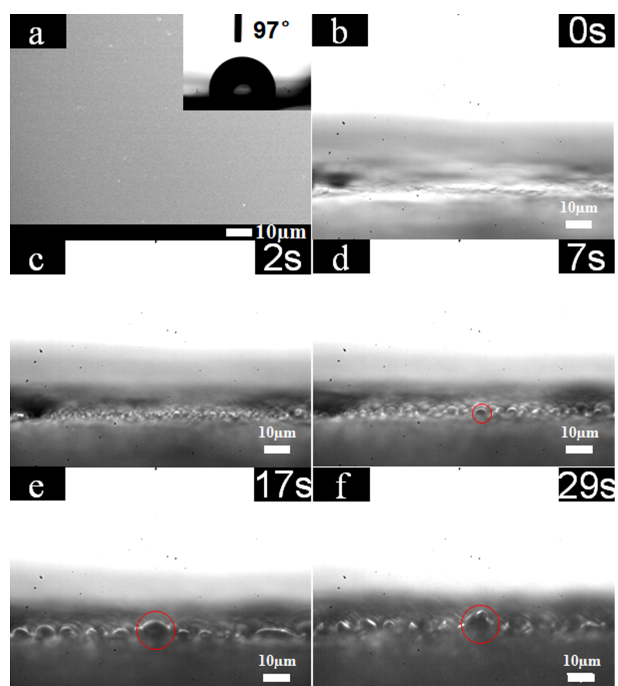


Fig. S2. (a) Scan Electronic Microscope (SEM) image of the hydrophobic i-PP film and (b~f) the optic photographs of frost formation on this i-PP film at -14 °C and RH 30% . The insert in (a) is the profile of a water droplet on the hydrophobic film.

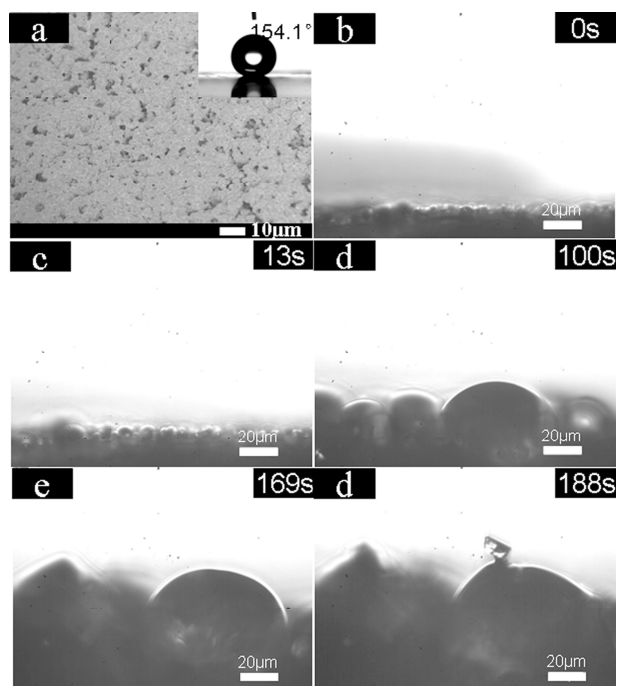


Fig. S3. (a) SEM image of the super-hydrophobic i-PP film and (b~f) the optic photographs of frost formation on this i-PP film at $-14\text{ }^\circ\text{C}$ and RH 30%. The insert in (a) is the profile of a water droplet on the super-hydrophobic film.

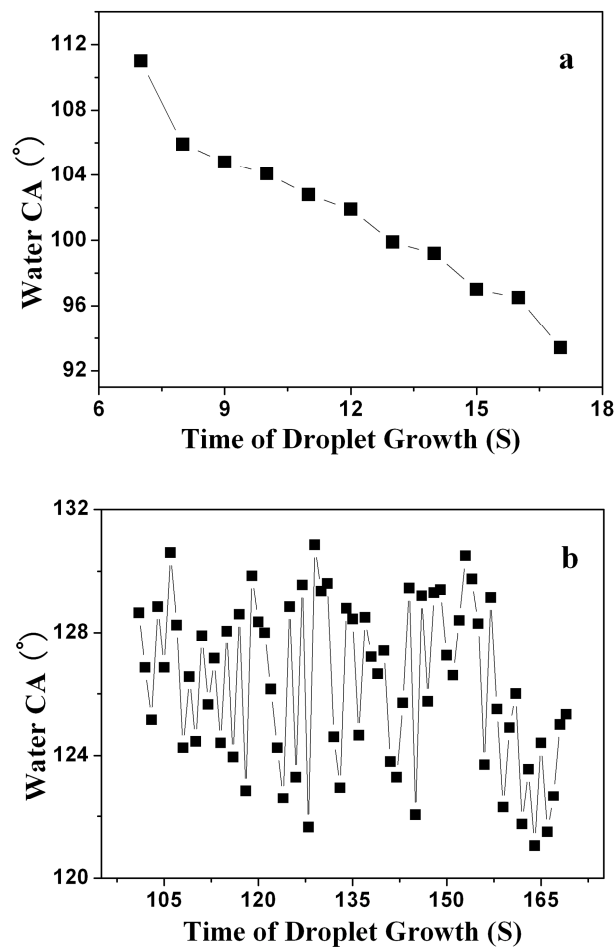


Fig. S4. Change of the water CA with growth time of the typical droplet in Fig. S2 (d-e) on (a) the hydrophobic i-PP surface and (b) the super-hydrophobic surface (-14 °C and RH 30%). The typical droplet corresponds to that in the Fig. S2 (d-e) (marked with red cycles) and the Fig. S3 (d-e), respectively.

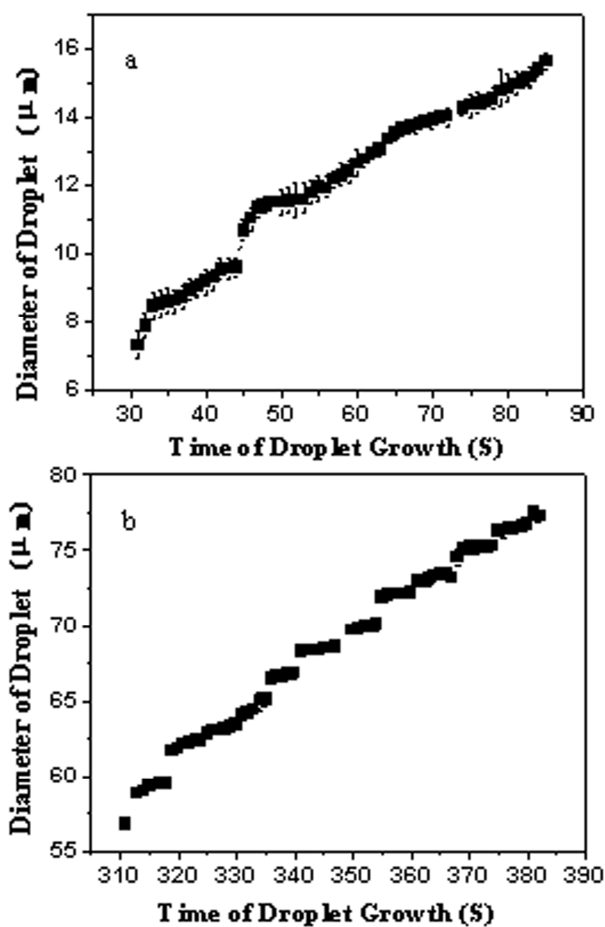


Fig. S5. Diameter of the typical droplet with growth time: (a) on the hydrophobic i-PP surface and (b) on the super-hydrophobic surface. The typical droplet corresponds to that in the Fig. 1 (d-e) (marked with red cycles) and the Fig. 2 (d-e), respectively.